European Journal of Medicinal Chemistry 84 (2014) 537–544

Contents lists available at ScienceDirect

European Journal of Medicinal Chemistry

journal homepage: http://www.elsevier.com/locate/ejmech

Original article

Metal complexes with 2-acetylpyridine-*N*(**4**)-*ortho*chlorophenylthiosemicarbazone: Cytotoxicity and effect on the enzymatic activity of thioredoxin reductase and glutathione reductase

Gabrieli L. Parrilha [a], Karina S.O. Ferraz [a], Josane A. Lessa [b], Kely Navakoski de Oliveira [c], Bernardo L. Rodrigues [a], Jonas P. Ramos [d], Elaine M. Souza-Fagundes [d], Ingo Ott [c, *], Heloisa Beraldo [a, *]

[a] Departamento de Química, Universidade Federal de Minas Gerais, 31270-901, Belo Horizonte, MG, Brazil
[b] Departamento de Química Geral e Inorgânica, Instituto de Química, Universidade do Estado do Rio de Janeiro, 20550-013, Rio de Janeiro, RJ, Brazil
[c] Institute of Medicinal and Pharmaceutical Chemistry, Technische Universität Braunschweig, Beethovenstrasse 55, 38106 Braunschweig, Germany
[d] Departamento de Fisiologia e Biofísica, Universidade Federal de Minas Gerais, 31270-901, Belo Horizonte, MG, Brazil

ARTICLE INFO

Article history:
Received 8 January 2014
Received in revised form
15 July 2014
Accepted 17 July 2014
Available online 17 July 2014

Keywords:
Thiosemicarbazones
Metal complexes
Thioredoxin reductase
Glutathione reductase
Anticancer drugs

ABSTRACT

Metal complexes with 2-acetylpyridine-*N*(4)-*ortho*chlorophenylthiosemicarbazone (H2Ac4*o*ClPh) were assayed for their cytotoxicity against MCF-7 breast adenocarcinoma and HT-29 colon carcinoma cells. The thiosemicarbazone and most of the complexes were highly cytotoxic. H2Ac4*o*ClPh and its gallium(III) and tin(IV) complexes did not show any inhibitory activity against thioredoxin reductase (TrxR) and glutathione reductase (GR). The palladium(II), platinum(II) and bismuth(III) complexes inhibited TrxR at micromolar concentrations but not GR. The antimony(III) and gold(III) complexes strongly inhibited TrxR at submicromolar doses with GR inhibition at higher concentrations. The selectivity of these complexes for TrxR suggests metal binding to a selenol residue in the active site of the enzyme. TrxR inhibition is likely a contributing factor to the mode of action of the gold and antimony derivatives.

1. Introduction

Cancer is a leading cause of mortality worldwide and the second leading cause of death in developing countries [1]. Surgery and radiotherapy dominated cancer treatment until the 1960s. Later, it became clear that survival rates increased by the use of combination chemotherapy, which opened up the opportunity to apply drugs in conjunction with surgery and/or radiation treatments [2].

The modern era of metal-based anticancer drugs began with the discovery of the antitumor properties of *cis*[diaminedichloroplatinum(II)], cisplatin. Currently, cisplatin and its successors carboplatin and oxaliplatin are among the most important chemotherapeutics used against a variety of cancers. However, side effects, drug resistance and treatment failure still pose great challenges in chemotherapy with platinum complexes [3].

Stimulated by the success of the platinum anticancer agents, other metal-based compounds are being tested for their antineoplastic activities. The literature reports a variety of metal complexes which present cytotoxic or antitumor activities, such as gallium(III) [4], gold(I,III) [5], antimony(III) [6], bismuth(III) [6] and ruthenium(II) complexes [7]. Much effort is directed to the search of the mechanism of action of non-platinum metal-based drug candidates and of their preferential protein targets since it became clear that DNA is not the target or the primary target for these compounds [8].

Thioredoxin reductase (TrxR) is a seleno-enzyme which is responsible for the nicotinamide adenine dinucleotide phosphate (NADPH) dependent reduction of its substrate thioredoxin (Trx) and many other oxidized cell constituents. It is involved in numerous metabolic pathways (e.g. antioxidant network, nucleotide biosynthesis) and pathophysiological conditions (tumors, infectious diseases, rheumatoid arthritis, etc) [9]. Auranofin exhibits *in vitro* cytotoxic activity and potently inhibits the enzymatic activity of TrxR. It has been shown that auranofin inhibits TrxR with approximately 1000-fold selectivity compared to the related enzymes glutathione reductase (GR) and glutathione peroxidase (GP)

* Corresponding authors.
E-mail addresses: hberaldo@ufmg.br, heloisaberaldoufmg@gmail.com (H. Beraldo).

http://dx.doi.org/10.1016/j.ejmech.2014.07.055
0223-5234/

[10]. In addition, based on numerous experimental evidences it has been proposed that the relevant cytotoxic actions produced by a variety of gold(I) and gold(III) compounds are mainly the result of potent TrxR inhibition [11], indicating that the main target of gold complexes is TrxR. Moreover, TrxR inhibition has also been observed with metal complexes different from gold [12]. This includes, for example, ruthenium or tin species [13–15].

Thiosemicarbazones have shown significant antineoplastic activity against a large number of human tumor cell lines under *in vitro* conditions [16]. α(*N*)-Heterocyclic thiosemicarbazones have been extensively investigated for their anticancer activity, which has been attributed to the inhibition of ribonucleoside diphosphate reductase (RDR), an essential enzyme involved in the conversion of ribonucleotides into deoxyribonucleotides during DNA syntheses [17].

Metal complexes with thiosemicarbazones also proved to be cytotoxic against several tumor cell lines. We demonstrated that gallium(III) [18,19], platinum(II), palladium(II) [20], gold(I) [21], antimony(III) [22], and tin(IV) [23] complexes with thiosemicarbazones show cytotoxic activity against human solid tumor and leukemia cell lines. The mode of action of the gallium(III) complexes might involve inhibition of RDR [4] while palladium(II) and platinum(II) complexes probably bind to DNA [20,24] and the gold(I) complexes act as TrxR inhibitors *in vitro* [21].

In previous works some of us demonstrated that 2-acetylpyridine-derived thiosemicarbazones are highly cytotoxic to human tumor cell lines. 2-Acetylpyridine *N*(4)-*ortho*-, *N*(4)-*meta* and *N*(4)-*para*-chlorophenyl thiosemicarbazone revealed to be cytotoxic at nanomolar doses against glioma cells with good therapeutic indexes and were able to induce cell death by apoptosis induction [25]. In addition, the thiosemicarbazones also proved to be cytotoxic at nanomolar doses against MCF-7 breast adenocarcinoma cells, the *ortho*-chloro derivative being particularly effective. Moreover, the thiosemicarbazones antitumoral doses resulted in no significant toxicity to red blood cells [26].

As mentioned before we had previously shown that gold(I) complexes with 2-acetylpyridine-derived thiosemicarbazones strongly inhibit TrxR activity *in vitro* [21]. In the present work we prepared gold(III), platinum(II), palladium(II), bismuth(III), tin(IV), antimony(III) and gallium(III) complexes with *N*(4)-*ortho*-chlorophenyl-2-acetylpyridine thiosemicarbazone (H2Ac4*o*ClPh) and assayed the compounds for their cytotoxic activity against MCF-7 breast adenocarcinoma and HT-29 colon carcinoma cells. The ability of the compounds under study to act as inhibitors of the enzymatic activities of TrxR and GR was investigated (Fig. 1).

2. Experimental

2.1. Physical measurements

All common chemicals were purchased from Aldrich and used without further purification. Partial elemental analyses were performed on a Perkin Elmer CHN 2400 analyzer. An YSI model 31 conductivity bridge was employed for molar conductivity measurements. Infrared spectra were recorded on a Perkin Elmer FT-IR Spectrum GX spectrometer using KBr plates (4000–400 cm^{-1}). NMR spectra were obtained with a Bruker DPX-200 Avance (200 MHz) spectrometer using DMSO-d_6 or MeOD-d_4 as solvent and TMS as internal reference.

2.2. Synthesis of N(4)-ortho-chlorophenyl-2-acetylpyridine thiosemicarbazone

N(4)-*ortho*-chlorophenyl-2-acetylpyridine thiosemicarbazone (H2Ac4*o*ClPh) was prepared as described in the literature [27]. IR and NMR data were compatible with the proposed structure.

2.3. Synthesis of the complexes

Dichloro[*N*(4)-*ortho*-chlorophenyl-2-acetylpyridinethiosemicarbazonato]antimony(III), [Sb(2Ac4*o*ClPh)Cl_2], (**1**) and *n*-butyldichloro[*N*(4)-*ortho*-chlorophenyl-2-acetylpyridinethiosemicarbazonato]tin(IV), [(*n*-Bu)Sn(2Ac4*o*ClPh)Cl_2], (**2**) were prepared as previously described [28,29].

The synthesis and characterization data of complex (**3**–**7**) are described below.

2.3.1. Bis[N(4)-ortho-chorophenyl-2-acetylpyridinethiosemicarbazonato]gallium(III) nitrate trihydrate, [Ga(2Ac4oClPh)$_2$]NO_3·3H_2O (**3**)

The complex was obtained by mixing a methanol solution (10 mL) of H2Ac4*o*ClPh (1.4 mmol) with gallium nitrate in a 2:1 ligand-to-metal molar ratio under reflux for 7 h. After cooling to room temperature and 24 h of stirring, the resulting solid was filtered, washed with methanol followed by diethyl ether, and dried *in vacuo*.

Yellow solid. Anal. Calc. for $C_{28}H_{30}Cl_2N_9O_6S_2Ga$ (FW = 793.36 g mol^{-1}): C, 42.39%, H, 3.81%, N, 15.89%. Found: C, 42.34%, H, 3.72%, N, 15.99%. Molar conductivity (1×10^{-3} mol L^{-1} DMF): 65.1 Ω^{-1} cm^2 mol^{-1}. IR (KBr, cm^{-1}): ν(C=N) 1591 s, ν(C–S) 780 m, ν (NO_3) 1428 s, 836 m, 683w, ρ(py) 651 m. The main signals in ^{1}H NMR (DMSO-d_6): δ(ppm) = 10.00 (1H, s, N(4)-H), 8.06 (1H, d, H6), 8.32–8.22 (2H, m, H3 and H4), 7.47–7.25 (1H, m, H5), 2.76 (3H, s, H15). The main signals in ^{13}C NMR (DMSO-d_6): δ (ppm) = 174.70 (C8), 150.09 (C2), 144.52 (C6), 144.83 (C7), 142.53 (C4), 124.55 (C3), 127.36 (C5), 14.49 (C15). Melting point: 172.7–174.8 °C. Yield: 38%.

2.3.2. Dihydroxo[N(4)-ortho-chlorophenyl-2-acetylpyridinethiosemicarbazonato]bismuth(III), [Bi(2Ac4oClPh)(OH)$_2$] (**4**)

The complex was obtained by mixing a methanol solution (10 mL) of H2Ac4*o*ClPh (0.7 mmol) with an equimolar amount of bismuth chloride under reflux for 7 h. After cooling to room temperature and 24 h of stirring, the resulting solid was filtered, washed with methanol followed by diethyl ether, and dried *in vacuo*.

Orange solid. Anal. Calc. for $C_{14}H_{14}ClN_4O_2SBi$ (FW = 546.79 g mol^{-1}): C, 30.75%, H, 2.58%, N, 10.25%. Found: C, 30.41%, H, 2.31%, N, 9.99%. Molar conductivity (1×10^{-3} mol L^{-1} DMF): 14.6 Ω^{-1} cm^2 mol^{-1}. IR (KBr, cm^{-1}): ν(C=N) 1590 s, ν(C–S) 778 m, ρ(py) 657 m. The main signals in ^{1}H NMR (MeOD-d_4): δ(ppm) = 8.46 (1H, d, H6), 8.78 (1H, d, H3), 8.69 (1H, t, H4), 8.05 (1H, t, H5), 2.55 (3H, s, H15). Melting point: 243.3–244.6 °C. Yield: 91%.

2.3.3. Chloro[N(4)-ortho-chlorophenyl-2-acetylpyridinethiosemicarbazonato]gold(III)dichloroaurate(I), [Au(2Ac4oClPh)Cl][$AuCl_2$] (**5**)

The complex was obtained by stirring under reflux a methanol solution (10 mL) of H2Ac4*o*ClPh (0.7 mmol) with an equimolar amount of sodium tetrachloroaurate(III) dihydrate for 1 h. The resulting solid was filtered, washed with methanol followed by diethyl ether, and dried *in vacuo*.

Red solid. Anal. Calc. for $C_{14}H_{12}Cl_4N_4SAu_2$ (FW = 804.08 g mol^{-1}): C, 20.91%, H, 1.50%, N, 6.97%. Found: C, 21.82%, H, 1.61%, N, 7.02%. Molar conductivity (1×10^{-3} mol L^{-1} DMF): 56.7 Ω^{-1} cm^2 mol^{-1}. IR (KBr, cm^{-1}): ν(C=N) 1588 s, ν(C–S) 760 m, ρ(py) 664 m. The main signals in ^{1}H NMR (MeOD-d_4): δ(ppm) = 8.27 (1H, d, H6), 9.04 (1H, d, H3), 8.51 (1H, t, H4), 8.02 (1H, t, H5), 2.64 (3H, s, H15). Melting point: 218.9–222.6 °C. Yield: 62%.

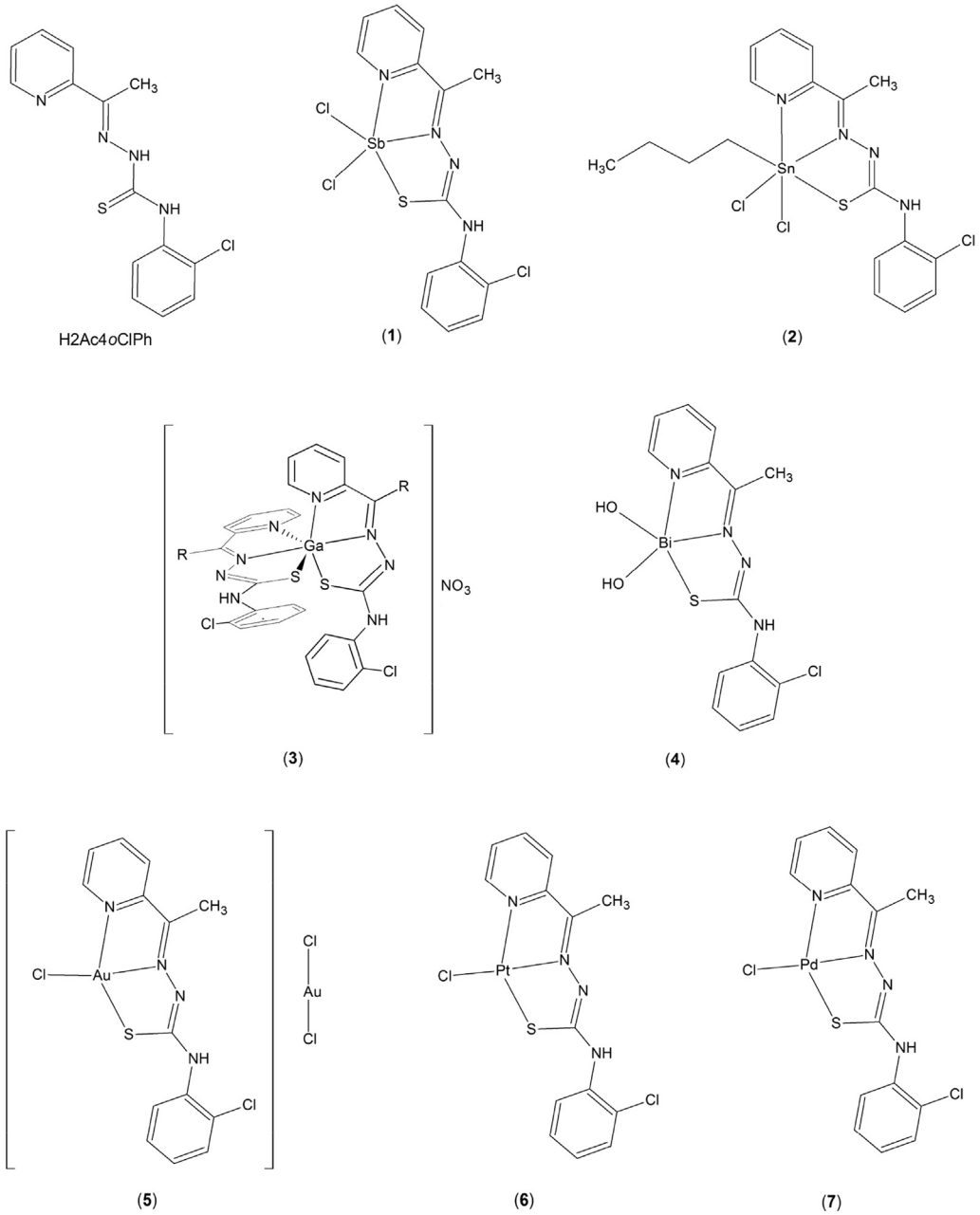

Fig. 1. Structure of 2-acetylpyridine-*N*(4)-*ortho*chlorophenyl thiosemicarbazone (H2Ac4oClPh) and its complexes [Sb(2Ac4oClPh)Cl_2] (**1**), [(*n*-Bu)Sn(2Ac4oClPh)Cl_2] (**2**), [Ga(2Ac4oClPh)$_2$]$NO_3 \cdot 3H_2O$ (**3**), [Bi(2Ac4oClPh)$(OH)_2$] (**4**), [Au(2Ac4oClPh)Cl]$AuCl_2$ (**5**), [Pt(2Ac4oClPh)Cl] (**6**) and [Pd(2Ac4oClPh)Cl] (**7**).

*2.3.4. Chloro[N(4)-ortho-chlorophenyl-2-acetylpyridinethiosemicarbazonato]platinum(II), [Pt(2Ac4oClPh)Cl] (**6**)*

The platinum complex was prepared by mixing under reflux an ethanol solution of H2Ac4oClPh (0.7 mmol) with an aqueous solution of K_2PtCl_4 in equimolar amounts for 2 h. The solid which precipitated was filtered off and washed with ethanol and ether, and dried *in vacuo*.

Red solid. Anal. Calc. for $C_{14}H_{12}Cl_2N_4SPt$ (FW = 534.32 g mol^{-1}): C, 31.47%; H, 2.26%; N, 10.49%. Found: C, 31.11%; H, 2.02%; N, 10.31%. Molar conductivity (1×10^{-3} mol L^{-1}, DMF): 5.4 Ω^{-1} cm^2 mol^{-1}. IR (KBr, cm^{-1}): ν(C═N) 1592 s, ν(C–S) 762 m, ρ(py) 668 m. The main signals in ^{1}H NMR (DMSO-d_6): δ(ppm) = 9.99 (1H, s, N(4)-H), 8.79 (1H, d, H6), 7.73–7.82 (2H, m, H4 and H5), 8.20 (1H, t, H4), 2.27 (3H, s, H15). The main signals in ^{13}C NMR (DMSO-d_6): δ (ppm) = 181.49 (C8), 157.92 (C2), 146.25 (C6), 159.36 (C7), 140.67 (C4), 125.89 (C3), 127.31 (C5), 13.27 (C15). Decomposes at 250 °C. Yield: 99%.

*2.3.5. Chloro[N(4)-ortho-chlorophenyl-2-acetylpyridinethiosemicarbazonato]palladium(II), [Pd(2Ac4oClPh)Cl] (**7**)*

The palladium(II) complex was prepared by mixing the desired ligand in ethanol with an aqueous solution of K_2PdCl_4 in equimolar amounts (0.7 mmol). The reaction mixture was kept under reflux for 2 h. The solid which precipitated was filtered off and washed with ethanol and ether, and then dried *in vacuo*.

Yellow solid. Anal. Calc. for $C_{14}H_{12}Cl_2N_4SPd$ (FW = 445.66 g mol^{-1}): C, 37.73%; H, 2.71%; N, 12.57%. Found: C, 37.76%; H, 2.62%; N, 12.53%. Molar conductivity (1×10^{-3} mol L^{-1}, DMF): 3.7 Ω^{-1} cm^2 mol^{-1}. IR (KBr, cm^{-1}): ν(C═N) 1592 s, ν(C–S)

766 m, ρ(py) 656 m. The main signals in ^{1}H NMR (DMSO-d_6): δ(ppm) = 9.87 (1H, s, N(4)-H), 8.55 (1H, d, H6), 7.85 (1H, d, H3), 8.18 (1H, t, H4), 7.66 (1H, t, H5), 2.30 (3H, s, H15). The main signals in ^{13}C NMR (DMSO-d_6): δ (ppm) = 180.04 (C8), 159.73 (C2), 149.66 (C6), 159.87 (C7), 142.75 (C4), 127.13 (C3), 129.18 (C5), 15.02 (C15). Decomposes at 280 °C. Yield: 97%.

2.4. X-ray diffraction analysis

X-ray data were collected at 293(2) K using MoKα (0.71073 Å) on an Agilent–Gemini diffractometer equipped with a CCD area detector. The CrysAlisPro software package [30] was used for data collection and data reduction. Data were corrected empirically for absorption using spherical harmonics and employing the SCALE3 ABSPACK [31] scaling algorithm. Data collected in the $4.2^{\circ} < \theta < 26.32^{\circ}$ interval were considered in the resolution and refinement of the structure. The structure was solved by direct methods using SHELXS-97 [32] and refined by full-matrix least squares on F^2 using SHELXL-97 [33]. All non-hydrogen atoms were successfully refined using anisotropic displacement parameters.

The thiosemicarbazone hydrogen atoms were geometrically fixed considering the hybridization of the parental atom. The occupations of the water solvent molecules were refined together with the water oxygen positions considering an isotropic displacement model for these atoms. The refinement indicates the presence of three water sites in the asymmetric unit. The sum of site occupancies suggests the presence of 0.81 water molecule in each asymmetric unit. Hence, although three hydration water molecules were suggested to be present in the powder, the crystal contained a different number of solvation molecules per asymmetric unit.

Crystallographic data for the structure were deposited in the Cambridge Crystallographic Data Centre, with number CCDC 974563.

2.5. Thioredoxin reductase and glutathione reductase inhibition assay

H2Ac4*o*ClPh and its complexes were investigated as inhibitors of rat liver TrxR and rat liver GR (both from Sigma–Aldrich) according to a method previously described [15,34]. In short: 25 μL of each compound solution [dimethylsulfoxide (DMSO) or dimethylformamide (DMF): 0.5% V/V] was incubated with 25 μL of each diluted enzyme (2.0–3.0 U/mL) in a 96-well plate with moderate shaking for 75 min at 37 °C. To each well, 200 μL of a mixture (1000 μL of mixture consisted of 500 μL of potassium phosphate buffer pH 7.0, 80 μL of EDTA solution 100 mM pH 7.5, 20 μL of bovinum serum albumin (BSA) solution 0.2% and 400 μL of distilled water), 25 μL of a 20 mM NADPH solution and finally 25 μL of a 20 mM ethanolic 5,5'-Dithiobis-(2-Nitrobenzoic Acid) (DTNB) solution were added. The formation of 5-thionitrobenzoic acid (5-TNB) over time was monitored with a microplate reader (Perkin–Elmer Victor X4) at 405 nm. The non interference of the compounds on the assay was confirmed by a negative control (enzyme-free solution of each tested compound). The IC_{50} was calculated as that concentration reducing the velocity of 5-TNB formation by 50%. Data were obtained in 2–3 independent experiments.

2.6. Cell culture and antiproliferative effects on MCF-7 and HT-29 cells

Antiproliferative effects of all compounds were evaluated against MCF-7 breast adenocarcinoma and HT-29 colon carcinoma cells. The cells were maintained in Dulbecco's Modified Eagle's Medium (DMEM) high glucose (PAA Laboratories) supplemented with 50 mg/L gentamycin and 10% (V/V) fetal calf serum (FCS) prior to use. DMSO/DMF compound solutions were diluted with cell culture medium (final concentration: 0.1% V/V DMSO or DMF) and were incubated with the cancer cells according to an established procedure (crystal violet assay) [34]. The IC_{50} value was described as the concentration reducing proliferation by 50% compared to untreated control cells. Results were calculated as means and error of 2–3 independent experiments.

2.7. Cytotoxicity against non-tumor cells (vero cells)

Cytotoxicity to mammalian non-tumor-cells was evaluated against vero (African green monkey kidney cells), as a representative of normal cells. This lineage was maintained in the logarithmic phase of growth in DMEM supplemented with 100 IU/mL penicillin and 100 μg/mL streptomycin enriched with 5% of fetal bovine serum and maintained at 37 °C in a humidified incubator with 5% CO_2 and 95% air. The medium was changed twice weekly and the cells were regularly examined and used until 20 passages.

Vero lineage was inoculated at 1×10^3 cells per well. The plates were pre-incubated for 24 h at 37 °C to allow adaptation of cells prior to the addition of the test compounds. All compounds were dissolved in dimethyl sulfoxide (DMSO, 0.5%) prior to dilution. The half maximal inhibitory concentration (IC_{50}) was determined over a range of concentrations (non-serial eight dilutions: from 100 to 0.00001 μM). The cells were incubated in a 5% CO_2/95% air-humidified atmosphere at 37 °C for 96 h. Negative control included treatment with 0.5% DMSO. Cell viability was estimated by measuring the rate of mitochondrial reduction of MTT (3-(4,5-dimethylthiazol-2-yl)-2,5-diphenyltetrazolium bromide). All samples were tested in triplicate, in at least two independent experiments [35]. The IC_{50} values for the cytotoxic activity were determined using Prism 5.0® (GraphPad Software Inc.).

3. Results and discussion

3.1. Formation of the complexes

Microanalyses and molar conductivity data are compatible with the formation of $[Ga(2Ac4oClPh)_2]NO_3 \cdot 3H_2O$ (**3**), $[Bi(2Ac4oClPh)(OH)_2]$ (**4**), $[Au(2Ac4oClPh)Cl][AuCl_2]$ (**5**), [Pt(2Ac4*o*ClPh)Cl] (**6**), and [Pd(2Ac4*o*ClPh)Cl] (**7**). In complex (**3**), two anionic thiosemicarbazones are attached to the metal center and one nitrate acts as counter-ion. In addition, solvation water molecules are present in **3**, as suggested by its infrared spectrum (see Section 3.2). $[Bi(2Ac4oClPh)(OH)_2]$ (**4**) is a neutral complex, containing one anionic thiosemicarbazone and two hydroxo ligands attached to the metal center. In **5** one anionic thiosemicarbazone and one chloride ion are attached to the gold(III) center and dichloroaurate(I) anion acts as counter-ion. Partial reduction of gold(III) to gold(I) took place in this case, as observed for other gold complexes with thiosemicarbazones [21,36]. Reduction of gold(III) by thiosemicarbazones could occur considering that these compounds exhibit reducing properties as shown by previous reports [37]. [Pt(2Ac4*o*ClPh)Cl] (**6**) and [Pd(2Ac4*o*ClPh)Cl] (**7**) are neutral complexes, in which an anionic thiosemicarbazone is attached to the metal center together with a chloride ion.

3.2. Spectroscopic characterization

The vibration attributed to ν(C=N) at 1581 cm^{-1} in the infrared spectrum of H2Ac4*o*ClPh shifts to 1592–1588 cm^{-1} in the spectra of its complexes (**3**–**7**), in agreement with coordination of the imine nitrogen [18,20]. The ν(CS) absorption observed at 809 cm^{-1} in the

spectrum of the free thiosemicarbazone shifts to 780–760 cm^{-1} in the spectra of the complexes, indicating coordination of the sulfur. The 29–49 cm^{-1} shift is compatible with complexation of a thiolate sulfur [38]. The in-plane deformation mode of the pyridine ring at 634 cm^{-1} in the spectrum of H2Ac4*o*ClPh shifts to 668–651 cm^{-1} in complexes (**3**–**7**), suggesting coordination of the hetero-aromatic nitrogen [18,28]. For complex (**3**), absorptions attributed to uncomplexed nitrate ion were observed at 1428 cm^{-1}, 836 cm^{-1} and 683 cm^{-1} and a broad absorption at 3650–3200 cm^{-1} was attributed to the ν(O–H) vibration [39].

The NMR spectra of H2Ac4*o*ClPh were recorded in both DMSO-d_6 and MeOD-d_4. The spectra of complexes (**3**), (**6**) and (**7**) were recorded in DMSO-d_6, whereas the spectra of **4** and **5** were recorded in MeOD-d_4. The ^{1}H resonances were assigned on the basis of chemical shifts and multiplicities. We could not obtain ^{13}C NMR spectra of H2Ac4*o*ClPh and complexes (**4**) and (**5**) in MeOD-d_4 due to their low solubility in this solvent. For **3**, **6** and **7**, the C-atom type (C, CH) was determined by using distortionless enhancement by polarization transfer (DEPT-135) experiments. The assignments of the protonated carbons were accomplished by 2D hetero-nuclear multiple quantum coherence experiments (HMQC).

The signals of all hydrogens are duplicated in the ^{1}H NMR spectrum of H2Ac4*o*ClPh recorded in DMSO-d_6, indicating the presence of the *E* (95%) and *Z* (5%) configurational isomers. The N(3)-H chemical shift at δ 10.90 ppm is characteristic of the *E* configuration, in which N(3)-H is hydrogen bonded to the solvent and the chemical shift at 14.70 ppm indicates *Z* configuration, in which N(3)-H is hydrogen bonded to the pyridine nitrogen [25]. Duplicated signals were not observed in the ^{13}C NMR spectrum of H2Ac4*o*ClPh, probably due to the low concentration of the *Z* isomer.

In the ^{1}H and ^{13}C NMR spectra of **3**, **6** and **7** only one signal was observed for each hydrogen and each carbon. The absence of the N(3)-H signal indicates coordination of the anionic thiosemicarbazone. The signals of all hydrogen atoms undergo significant shifts in relation to their positions in the free ligand. Similarly, the signals of C=N, C=S and the pyridine carbon atoms undergo significant shifts, indicating coordination of H2Ac4*o*ClPh through the N_{py}-N_{imine}-S chelating system. Hence in complexes (**3**), (**6**) and (**7**) the thiosemicarbazone adopts the *E* configuration.

In the ^{1}H NMR spectrum of H2Ac4*o*ClPh recorded in MeOD-d_4, the signals are also duplicated due to the presence of the *E* and *Z* configurational isomers, while only one signal was observed for each hydrogen in the NMR spectra of **4** and **5**. The signals of N(3)-H were absent in the spectra of **4** and **5**, in accordance with the presence of an anionic ligand upon deprotonation. In addition, the signals of all hydrogen atoms undergo significant shifts in relation to their positions in the free thiosemicarbazone.

3.3. X-ray diffraction analysis

Crystals of [Ga(2Ac4*o*ClPh)$_2$]NO_3·0.81H_2O (**3a**) were obtained upon dissolution of complex (**3**) in DMSO. The atom arrangements and atom numbering scheme for **3a** are shown in Fig. 2, while crystal data and refinement results are listed in Table 1. The crystal structure of H2Ac4*o*ClPh has been previously determined by some of us [25]. Tables 2 and 3 present selected bond angles and intramolecular bond distances for H2Ac4*o*ClPh [25] and complex (**3a**).

In **3a** gallium(III) is in a distorted octahedral environment, coordinated to two tridentate anionic thiosemicarbazones. The sulfur atoms are in *cis* position to each other and *trans* to the pyridine nitrogen, while the imine N-atoms are in *trans* position to each other. *Trans* L-Ga-L angles are in the range from 158.19(8) to 172.53(12)° and *cis* L-Ga-L angles from 76.80(11) to 103.58(9)°.

H2Ac4*o*ClPh crystallizes in the *EE* conformation [25], whilst in complex (**3a**) the thiosemicarbazones adopt the *EZ* conformation.

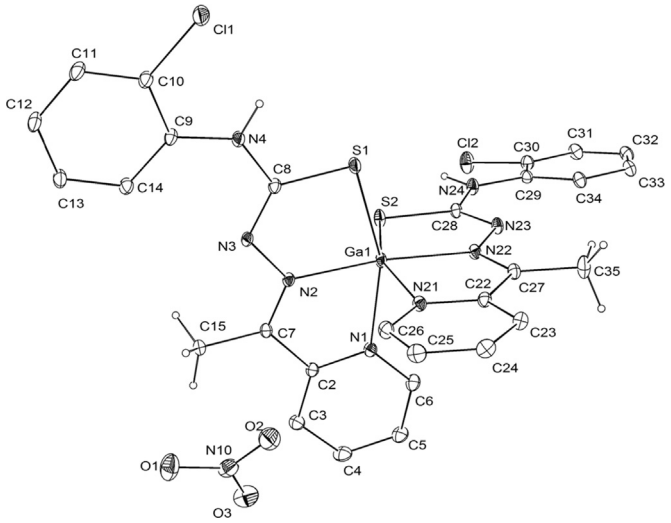

Fig. 2. Atom arrangements and atom numbering for [Ga(2Ac4*o*ClPh)$_2$]NO_3·0.81H_2O (**3a**).

The same behavior had also been observed for [Ga(2Ac4Ph)$_2$]NO_3·0.5H_2O [40]. Hence, some angles undergo significant changes upon coordination. The N(2)–N(3)–C(8) angle goes from 118.2(2) and 118.9(2)° in H2Ac4*o*ClPh [25] to 113.1(3) and 113.3(3)° in **3a**. The N(4)–C(8)–S(1) angle varies from 124.3(2) and 124.1(2)° in H2Ac4*o*ClPh [25] to 113.4(3) and 113.7(3)° in complex (**3a**).

There is a slight shortening of the bond distance between gallium(III) and the imine nitrogen (2.054(3) and 2.058(3) Å) compared to the distance between gallium(III) and the hetero-aromatic nitrogen (2.120(3) and 2.121(3) Å). Similar features were observed in other complexes with thiosemicarbazones [19,40]. The Ga–S distances are 2.3703(10) and 2.3663(11) Å.

Table 1
Crystal data and structure refinement for [Ga(2Ac4*o*ClPh)$_2$]NO_3·0.81H_2O (**3a**).

Compound	[Ga(2Ac4*o*ClPh)$_2$]NO_3·0.81H_2O (**3a**)
Empirical formula	C28 H25.6 Cl2 Ga N9 O3.81 S2
Formula weight (g mol^{-1})	753.92
Temperature (K)	293 (2)
Wavelength (Å)	0.71073
Crystal system, space group	P-1, triclinic
Crystal size (mm^3)	0.11 × 0.12 × 0.15
a (Å)	10.9156 (5)
b (Å)	12.3807 (6)
c (Å)	14.1920 (8)
Unit cell dimensions	
α (°)	66.763 (5)
β (°)	76.521 (4)
γ (°)	78.095 (4)
Volume ($Å^3$)	1699.74 (15)
Z, Calculated density Mg m^{-3}	2, 1.473
Absorption coefficient mm^{-1}	1.136
F (000)	768.2
θ range for data collection (°)	1.92 to 29.99
Limiting indices	$-14 \le h \le 15$ $-16 \le k \le 15$ $-19 \le l \le 17$
Reflections collected/unique (R_{int})	29046/8413 (0.0472)
Completeness	θ = 26.32° 99.97%
Absorption correction	Empirical
Refinement method	Full-matrix least-squares on F^2
Data/restraints/parameters	8413/0/423
Goodness-of-fit on F^2	1.019
Final *R* indices [$I > 2\sigma(I)$]	$R1$ = 0.0574, w$R2$ = 0.1686
R indices (all data)	$R1$ = 0.0839, w$R2$ = 0.1937
Largest diff. peak and hole (e $Å^{-3}$)	1.019 and −0.717

Table 2
Selected angles (°) for H2Ac4*o*ClPh [25] and [Ga(2Ac4*o*ClPh)$_2$]NO$_3$·0.81H$_2$O (**3a**).

Atoms	H2Ac4*o*ClPh [25][a]		Atoms	**3a**
C(7)-N(2)-N(3)	119.1 (2)	118.7 (2)	C(7)-N(2)-N(3)	117.7 (3)
			C(27)-N(22)-N(23)	118.4 (3)
N(2)-N(3)-C(8)	118.2 (2)	118.9 (2)	N(2)-N(3)-C(8)	113.1 (3)
			N(22)-N(23)-N(28)	113.3 (3)
N(3)-C(8)-S(1)	121.0 (2)	121.5 (2)	N(3)-C(8)-S(1)	127.1 (3)
			N(23)-C(28)-S(2)	127.2 (3)
N(3)-C(8)-N(4)	114.7 (2)	114.4 (2)	N(3)-C(8)-N(4)	119.5 (3)
			N(23)-C(28)-N(24)	119.1 (3)
N(4)-C(8)-S(1)	124.3 (2)	124.1 (2)	N(4)-C(8)-S(1)	113.4 (3)
			N(24)-C(28)-S(2)	113.7 (3)
–	–	–	N(1)-Ga(1)-N(2)	76.80 (11)
–	–	–	N(21)-Ga(1)-N(22)	76.81 (12)
–	–	–	N(1)-Ga(1)-S(1)	158.19 (8)
–	–	–	N(21)-Ga(1)-S(2)	158.34 (8)
–	–	–	N(2)-Ga(1)-S(1)	81.75 (8)
–	–	–	N(22)-Ga(1)-S(2)	81.97 (9)
–	–	–	N(1)-Ga(1)-N(21)	86.91 (12)
–	–	–	N(1)-Ga(1)-N(22)	98.21 (12)
–	–	–	N(1)-Ga(1)-S(2)	91.88 (9)
–	–	–	N(2)-Ga(1)-N(21)	97.20 (11)
–	–	–	N(2)-Ga(1)-N(22)	172.53 (12)
–	–	–	N(2)-Ga(1)-S(2)	103.58 (9)
–	–	–	S(1)-Ga(1)-N(21)	91.91 (9)
–	–	–	S(1)-Ga(1)-N(22)	102.72 (9)
–	–	–	S(1)-Ga(1)-S(2)	97.00 (4)

[a] There are two molecules in the asymmetric unit.

The expected lengthening of the C(8)–S(1) bond from 1.654(3) Å in H2Ac4*o*ClPh [25] to 1.742(3) and 1.743(3) Å in **3a**, and shortening of the N(3)–C(8) bond from 1.359(3) and 1.351(3) Å in H2Ac4*o*ClPh [25] to 1.315(5) and 1.309(5) Å in **3a** were observed. Therefore, the C(8)–S(1) bond changes from double to a predominantly single bond whereas N(3)–C(8) acquires some double bond character due to deprotonation at N(3) and formation of a highly delocalized system.

3.4. Enzyme inhibition

The IC$_{50}$ values of compounds for TrxR and GR inhibition and antiproliferative activity against HT-29 and MCF-7 cells are listed in Table 4. The studied compounds presented distinct effects on the enzymatic activity of TrxR and GR. Indeed, the thiosemicarbazone ligand, although being highly cytotoxic against the two cell lines at nanomolar doses, does not show any inhibitory activity against TrxR and GR. The main target of thiosemicarbazones is believed to be RDR [17]. The same behavior was observed for the gallium(III) and tin(IV) complexes.

RDR is also believed to be the main target of gallium(III) complexes. In fact, since gallium(III) and iron(III) show very similar charge-to-radius ratio, the chemical behavior of gallium(III) closely resembles that of iron(III). Gallium resemblance to iron allows its interaction with cellular processes and important proteins of iron metabolism. Due to competitive binding of gallium(III) and iron(III), gallium affects intracellular iron availability, but it also interacts directly with RDR, displacing iron from the enzyme [4]. Although it has been suggested that the antiproliferative effects of organotin(IV) compounds are related to metal binding to thiol groups of proteins, the mode of cytotoxic action of these compounds remains largely unknown [41]. In a previous work TrxR inhibition by di and triorganotin(IV) carboxilates was demonstrated [15]. However in the present work complex (**2**) was unable to inhibit both TrxR and GR enzymatic activities under the experimental conditions.

The palladium(II), platinum(II) and bismuth(III) complexes inhibited TrxR at micromolar concentrations but not GR (IC$_{50}$ values > 100 μM). Both the antimony (**1**) and gold (**5**) complexes strongly inhibited TrxR at submicromolar dosages with GR inhibition at much higher concentrations. TrxR and GR are flavoproteins of the same family that provide reducing equivalents to many cellular processes. Since only TrxR is a selenoprotein [42], the selectivity of these complexes for TrxR may suggest metal binding to a selenol residue in the active site of the enzyme. Comparing the TrxR inhibition results with those of the cytotoxicity studies a correlation could not be established, which is in agreement with previous studies [43]. However, due to their low IC$_{50}$ values TrxR inhibition is likely a contributing factor for the cytotoxic effect in particular of the gold(III) and antimony(III) derivatives.

3.5. Cytotoxic activity

The cytotoxic effects (IC$_{50}$) of the studied compounds are listed in Table 4. The metal free H2Ac4*o*ClPh is cytotoxic to both MCF-7 and HT-29 cell lines at nanomolar doses. However, the metal salts used as starting material for the synthesis are not active with the exception of $SbCl_3$ and $NaAuCl_4 \cdot 2H_2O$ (data not shown). In general coordination either results in a slight improvement of activity or does not appreciably change cytotoxicity except in the cases of complexes (**6**) and (**7**) which showed a lower cytotoxic effect than the uncomplexed thiosemicarbazone against both cell lineages.

Cytotoxicity was evaluated against vero cells, as a representative of normal cells (see Table 4). The results suggest that most of the compounds under study were less cytotoxic to vero than to the assayed tumor cell lineages.

Table 3
Selected intramolecular bond distances (Å) for H2Ac4*o*ClPh [25] and [Ga(2Ac4*o*ClPh)$_2$]NO$_3$·0.81H$_2$O (**3a**).

Atoms	H2Ac4*o*ClPh [25][a]		Atoms	**3a**
N(2)-C(7)	1.281 (3)	1.278 (3)	N(2)-C(7)	1.295 (5)
			N(22)-C(27)	1.294 (5)
N(2)-N(3)	1.362 (3)	1.361 (3)	N(2)-N(3)	1.371 (4)
			N(22)-N(23)	1.376 (4)
N(3)-C(8)	1.359 (3)	1.351 (3)	N(3)-C(8)	1.315 (5)
			N(23)-C(28)	1.309 (5)
N(4)-C(8)	1.328 (4)	1.336 (3)	N(4)-C(8)	1.361 (5)
			N(24)-C(28)	1.358 (5)
C(8)-S(1)	1.654 (3)	1.654 (3)	C(8)-S(1)	1.742 (3)
			C(28)-S(2)	1.743 (3)
–	–	–	Ga(1)-N(1)	2.121 (3)
–	–	–	Ga(1)-N(21)	2.120 (3)
–	–	–	Ga(1)-N(2)	2.054 (3)
–	–	–	Ga(1)-N(22)	2.058 (3)
–	–	–	Ga(1)-S(1)	2.3703 (10)
–	–	–	Ga(1)-S(2)	2.3663 (11)

[a] There are two molecules in the asymmetric unit.

4. Conclusions

H2Ac4*o*ClPh and its antimony(III), tin(IV), gallium(III), bismuth(III) and gold(III) complexes proved to be highly cytotoxic to MCF-7 and HT29 cells whereas the palladium(II) and platinum(II) complexes were not as effective. The mechanisms of the cytotoxic effect for these compounds are probably very distinct. While the free thiosemicarbazone and its gallium(III) and tin(IV) complexes did not inhibit either TrxR or GR, the bismuth(III), palladium(II) and platinum(II) were able to inhibit TrxR but not GR. The antimony(III) and gold(III) complexes were able to inhibit both enzymes but were much stronger inhibitors of TrxR. The selectivity of these complexes for TrxR suggests that binding to a selenol residue in the active site of the enzyme is probably part of their mode of action. Overall the cytotoxic effect of the compounds is largely the result of the coordinated thiosemicarbazone ligand. However, selective inhibition of

Table 4
IC_{50} values of compounds for TrxR and GR inhibition and cytotoxic activity against HT-29, MCF-7 and Vero cells.

Compounds	Enzyme inhibition (IC_{50}, μmol L^{-1})		Cytotoxic effect (IC_{50}, μmol L^{-1})		
	TrxR	GR	MCF-7	HT-29	Vero
H2Ac4*o*ClPh	>100	>100	$7.02 \pm 1.14 \times 10^{-3}$	$6.96 \pm 1.28 \times 10^{-3}$	0.02 ± 0.01
[Sb(2Ac4*o*ClPh)Cl_2] (**1**)	0.16 ± 0.03	37.71 ± 5.11	$3.55 \pm 1.07 \times 10^{-3}$	$4.75 \pm 0.75 \times 10^{-3}$	0.13 ± 0.11
[(*n*-Bu)Sn(2Ac4*o*ClPh)Cl_2] (**2**)	>100	>100	$4.60 \pm 0.64 \times 10^{-3}$	$5.23 \pm 0.43 \times 10^{-3}$	0.10 ± 0.04
[Ga(2Ac4*o*ClPh)$_2$]$NO_3 \cdot 3H_2O$ (**3**)	>100	>100	$3.56 \pm 0.44 \times 10^{-3}$	$1.84 \pm 0.37 \times 10^{-3}$	0.02 ± 0.01
[Bi(2Ac4*o*ClPh)(OH)$_2$] (**4**)	7.35 ± 2.68	>100	$4.30 \pm 1.63 \times 10^{-3}$	$6.16 \pm 0.72 \times 10^{-3}$	0.02 ± 0.01
[Au(2Ac4*o*ClPh)Cl][$AuCl_2$] (**5**)	0.23 ± 0.02	1.22 ± 0.09	$10.20 \pm 0.42 \times 10^{-3}$	$35.89 \pm 3.47 \times 10^{-3}$	0.09 ± 0.01
[Pt(2Ac4*o*ClPh)Cl] (**6**)	1.57 ± 1.32	>100	8.16 ± 2.74	2.87 ± 2.32	14.44 ± 0.98
[Pd(2Ac4*o*ClPh)Cl] (**7**)	9.73 ± 1.50	>100	1.38 ± 0.95	2.00 ± 0.93	2.84 ± 0.99

TrxR adds another mechanism contributing to their pharmacological profile. The complexes might thus provide prototypes for multitarget metallodrugs for cancer chemotherapy. Further structural optimization and elucidation of relevant pathways are certainly of interest. The identification of TrxR as a target for gold(III) and antimony(III) complexes might hopefully lead to the discovery of more effective, "mechanism-oriented", anticancer metallodrugs. In addition, to our knowledge this is the first report on inhibition of TrxR by an antimony(III) compound.

Acknowledgments

This work was supported by CNPq (Proc. 472305/2012-3), INCT-INOFAR (Proc. CNPq 988573.364/2008-6), CAPES-PNPD, and FAPEMIG.

Appendix A. Supplementary data

Supplementary data related to this article can be found at http://dx.doi.org/10.1016/j.ejmech.2014.07.055. These data include MOL files and InChIKeys of the most important compounds described in this article.

References

[1] A. Jemal, F. Bray, M.M. Center, J. Ferlay, E. Ward, D. Forman, Global cancer statistics, CA Cancer J. Clin. 61 (2011) 69–90.
[2] V.T. DeVita, E. Chu, A history of cancer chemotherapy, Cancer Res. 68 (2008) 8643–8653.
[3] B. Lippert (Ed.), Cisplatin. Chemistry and Biochemistry of a Leading Anticancer Drug, Wiley-VCH, Weinheim, 1999.
[4] J.A. Lessa, G.L. Parrilha, H. Beraldo, Gallium complexes as new promising metallodrug candidates, Inorg. Chim. Acta 393 (2012) 53–63 (and references therein).
[5] S. Nobili, E. Mini, I. Landini, C. Gabbiani, A. Casini, L. Messori, Gold compounds as anticancer agents: chemistry, cellular pharmacology, and preclinical studies, Med. Res. Rev. 30 (2010) 550–580.
[6] E.R.T. Tiekink, Antimony and bismuth compounds in oncology, Crit. Rev. Onc. Hemat. 42 (2002) 217–224.
[7] L. Bratsos, S. Jedner, T. Gianferrara, E. Alessio, Ruthenium anticancer compounds: challenges and expectations, Chimia 61 (2007) 692–697.
[8] C. Gabbiani, G. Mastrobuoni, F. Sorrentino, B. Dani, M.P. Rigobello, A. Bindoli, M.A. Cinellu, G. Pieraccini, L. Messoria, A. Casini, Thioredoxin reductase, an emerging target for anticancer metallodrugs. Enzyme inhibition by cytotoxic gold(III) compounds studied with combined mass spectrometry and biochemical assays, Med. Chem. Commun. 2 (2011) 50–54.
[9] K. Becker, S. Gromer, R.H. Schirmer, S. Müller, Thioredoxin reductase as a pathophysiological factor and drug target, Eur. J. Biochem 267 (2000) 6118–6125.
[10] I. Ott, On the medicinal chemistry of gold complexes as anticancer drugs, Coord. Chem. Rev. 253 (2009) 1670–1681.
[11] A. Bindoli, M.P. Rigobello, G. Scutari, C. Gabbiani, A. Casini, L. Messori, Thioredoxin reductase: a target for gold compounds acting as potential anticancer drugs, Coord. Chem. Rev. 253 (2009) 1692–1707.
[12] W. Cai, L. Zhang, Y. Song, B. Wang, B. Zhang, X. Cui, G. Hu, Y. Liu, J. Wu, J. Fang, Small molecule inhibitors of mammalian thioredoxin reductase, Free Radic. Biol. Med. 52 (2012) 257–265.
[13] P. Mura, M. Camalli, A. Bindoli, F. Sorrentino, A. Casini, C. Gabbiani, M. Corsini, P. Zanello, M.P. Rigobello, L. Messori, Activity of rat cytosolic thioredoxin reductase is strongly decreased by *trans*-[bis(2-amino-5-methylthiazole)tetrachlororuthenate(III)]: first report of relevant thioredoxin reductase inhibition for a ruthenium compound, J. Med. Chem. 50 (2007) 5871–5874.
[14] L. Oehninger, M. Stefanopoulou, H. Alborzinia, J. Schur, S. Ludewig, K. Namikawa, A. Munoz-Castro, R.W. Köster, K. Baumann, S. Wölfl, W.S. Sheldrick, I. Ott, Evaluation of arene ruthenium(II) *N*-heterocyclic carbene complexes as organometallics interacting with thiol and selenol containing biomolecules, Dalt. Trans. 42 (2013) 1657–1666.
[15] K.N. de Oliveira, V. Andermark, S. von Grafenstein, L.A. Onambele, G. Dahl, R. Rubbiani, G. Wolber, C. Gabbiani, L. Messori, A. Prokop, I. Ott, Butyltin(IV) benzoates: inhibition of thioredoxin reductase, tumor cell growth inhibition, and interactions with proteins, ChemMedChem 8 (2013) 256–264.
[16] H. Beraldo, D. Gambino, The wide pharmacological versatility of semicarbazones, thiosemicarbazones and their metal complexes, Mini Rev. Med. Chem. 4 (2004) 31–39.
[17] A. Popović-Bijelić, C.R. Kowol, M.E.S. Lind, J. Luo, F. Himo, E.A. Enyedy, V.B. Arion, A. Gräslund, Ribonucleotide reductase inhibition by metal complexes of triapine (3-aminopyridine-2-carboxaldehyde thiosemicarbazone): a combined experimental and theoretical study, J. Inorg. Biochem. 105 (2011) 1422–1431 (and references therein).
[18] J.A. Lessa, M.A. Soares, R.G. dos Santos, I.C. Mendes, L.B. Salum, H.N. Daghestani, A.D. Andricopulo, B.W. Day, A. Vogt, H. Beraldo, Gallium(III) complexes with 2-acetylpyridine-derived thiosemicarbazones: antimicrobial and cytotoxic effects and investigation on the interactions with tubulin, Biometals 26 (2013) 151–165.
[19] I.C. Mendes, M.A. Soares, R.G. dos Santos, C. Pinheiro, H. Beraldo, Gallium(III) complexes of 2-pyridineformamide thiosemicarbazones: cytotoxic activity against malignant glioblastoma, Eur. J. Med. Chem. 44 (2009) 1870–1877.
[20] K.O.S. Ferraz, G.M.M. Cardoso, C.M. Bertollo, E.M. Souza-Fagundes, N. Speziali, C.L. Zani, I.C. Mendes, M.A. Gomes, H. Beraldo, *N*(4)-tolyl-2-benzoylpyridine-derived thiosemicarbazones and their palladium(II) and platinum(II) complexes: cytotoxicity against human solid tumor cells, Polyhedron 30 (2011) 315–321.
[21] J.A. Lessa, J.C. Guerra, L.F. de Miranda, C.F.D. Romeiro, J.G. Da Silva, I.C. Mendes, N.L. Speziali, E.M. Souza-Fagundes, H. Beraldo, Gold(I) complexes with thiosemicarbazones: cytotoxicity against human tumor cell lines and inhibition of thioredoxin reductase activity, J. Inorg. Biochem 105 (2011) 1729–1739.
[22] D.C. Reis, M.C.X. Pinto, E.M. Souza-Fagundes, S.M.S.V. Wardell, J.L. Wardell, H. Beraldo, Antimony(III) complexes with 2-benzoylpyridine-derived thiosemicarbazones: cytotoxicity against human leukemia cell lines, Eur. J. Med. Chem. 45 (2010) 3904–3910.
[23] A. Perez-Rebolledo, J.D. Ayala, G.M. de Lima, N. Marchini, G. Bombieri, C.L. Zani, E.M. Souza-Fagundes, H. Beraldo, Structural studies and cytotoxic activity of N(4)-phenyl-2-benzoylpyridine thiosemicarbazone Sn(IV) complexes, Eur. J. Med. Chem. 40 (2005) 467–472.
[24] K.S.O. Ferraz, L. Ferandes, D. Carrilho, M.C.X. Pinto, M.F. Leite, E.M. Souza-Fagundes, N.L. Speziali, I.C. Mendes, H. Beraldo, 2-Benzoylpyridine-*N*(4)-tolyl thiosemicarbazones and their palladium(II) complexes: cytotoxicity against leukemia cells, Bioorg. Med. Chem. 17 (2009) 7138–7144.
[25] J.A. Lessa, I.C. Mendes, J.G. Da Silva, P.R.O. da Silva, M.A. Soares, R.G. dos Santos, N.L. Speziali, N.C. Romeiro, E.J. Barreiro, H. Beraldo, 2-Acetylpyridine thiosemicarbazones: cytotoxic activity in nanomolar doses against malignant gliomas, Eur. J. Med. Chem. 45 (2010) 5671–5677.
[26] M.A. Soares, J.A. Lessa, I.C. Mendes, J.G. Da Silva, R.G. Dos Santos, L.B. Salum, H. Daghestani, A.D. Andricopulo, B.W. Day, A. Vogt, J.L. Pesquero, W.R. Rocha, H. Beraldo, N4-Phenyl-substituted 2-acetylpyridine thiosemicarbazones: cytotoxicity against human tumor cells, structure–activity relationship studies and investigation on the mechanism of action, Bioorg. Med. Chem. 20 (2012) 3396–3409.
[27] M.C. Miller, C.N. Stineman, J.R. Vance, D.X. West, I.H. Hall, The cytotoxicity of copper(II) complexes of 2-acetyl-pyridil-4-*N*-substituted thiosemicarbazones, Anticancer Res. 18 (1998) 4131–4139 (and references therein).
[28] G.L. Parrilha, R.P. Dias, W.R. Rocha, I.C. Mendes, D. Benítez, J. Varela, H. Cerecetto, M. González, C.M.L. Melo, J.K.A.L. Neves, V.R.A. Pereira, H. Beraldo, 2-Acetylpyridine- and 2-benzoylpyridine-derived thiosemicarbazones and their antimony(III) complexes exhibit high antitrypanosomal activity, Polyhedron 31 (2012) 614–621.

[29] G.L. Parrilha, J.G. da Silva, L.F. Gouveia, A.K. Gasparoto, R.P. Dias, W.R. Rocha, D.A. Santos, N.L. Speziali, H. Beraldo, Pyridine-derived thiosemicarbazones and their tin(IV) complexes with antifungal activity against *Candida* spp. Eur. J. Med. Chem. 46 (2011) 1473–1482.
[30] CRYSALISPRO, Agilent Technologies, Version 1.171.35.21 (release 20-01-2012 CrysAlis171.NET).
[31] SCALE3 ABSPACK Scaling Algorithm CrysAlis, Agilent Technologies, Version 1.171.35.21 (release 20-01-2012 CrysAlis171NET).
[32] G.M. Sheldrick, SHELXS-97, Program for the Solution of Crystal Structures, University of Göttingen, Germany, 1997.
[33] G.M. Sheldrick, SHELXL-97, Program for the Refinement of Crystal Structures, University of Göttingen, Germany, 1997.
[34] R. Rubbiani, I. Kitanovic, H. Alborzinia, S. Can, A. Kitanovic, L.A. Onambele, M. Stefanopoulou, Y. Geldmacher, W.S. Sheldrick, G. Wolber, A. Prokop, S. Wölfl, I. Ott, Benzimidazol-2-ylidene gold(I) complexes are thioredoxin reductase inhibitors with multiple antitumor properties, J. Med. Chem. 53 (2010) 8608–8618.
[35] A. Monks, D. Scudiero, P. Skehan, R. Shoemaker, K. Paull, D. Vistica, C. Hose, J. Langley, P. Cronise, A. Vaigro-Wolff, Feasibility of a high-flux anticancer drug screen using a diverse panel of cultured human tumor cell lines, J. Nat. Cancer Inst. 83 (1991) 757–766.
[36] A. Sreeknth, H.K. Fun, M.R.P. Kurup, Formation of first gold(III) complex of an *N*(4)-disubstituted thiosemicarbazone derived from 2-benzoylpyridine: structural and spectral studies, Inorg. Chem. Commun. 7 (2004) 1250–1253.
[37] R.H.U. Borges, E. Paniago, H. Beraldo, Equilibrium and kinetic studies of iron(II) and iron(III) complexes of some α(*N*)-heterocyclic thiosemicarbazones. Reduction of the iron(III) complexes of 2-formylpyridine thiosemicarbazone and 2-acetylpyridine thiosemicarbazone by cellular thiol-like reducing agents, J. Inorg. Biochem. 65 (1997) 267–275.
[38] H. Beraldo, W.F. Nacif, L.R. Teixeira, J.S. Rebouças, Cobalt(II) and nickel(II) complexes of N(4′) substituted 3- and 4-acetylpyridine thiosemicarbazones, Transit. Metal. Chem. 27 (2002) 85–88.
[39] K. Nakamoto, Infrared Spectra of Inorganic and Coordination Compounds, fourth ed., Wiley, New York, 1986.
[40] J.G. Da Silva, L.S. Azzolini, S.M.S.V. Wardell, J.L. Wardell, H. Beraldo, Increasing the antibacterial activity of gallium(III) against *Pseudomonas aeruginosa* upon coordination to pyridine-derived thiosemicarbazones, Polyhedron 28 (2009) 2301–2305.
[41] S.K. Hadjikakou, N. Hadjiliadis, Antiproliferative and anti-tumor activity of organotin compounds Coord, Chem. Rev. 253 (2009) 235–249.
[42] A.B. Witte, K. Anestål, E. Jerremalm, H. Ehrsson, E.S.J. Arnér, Inhibition of thioredoxin reductase but not of glutathione reductase by the major classes of alkylating and platinum-containing anticancer compounds, Free Radic. Biol. Med. 39 (2005) 696–703.
[43] R. Rubbiani, E. Schuh, A. Meyer, J. Lemke, J. Wimberg, N. Metzler-Nolte, F. Meyer, F. Mohr, I. Ott, TrxR inhibition and antiproliferative activities of structurally diverse gold N-heterocyclic carbene complexes, MedChemComm 4 (2013) 942–948.